Membrane Water Treatment, Vol. 2, No. 3 (2011) 187-205
DOI: http://dx.doi.org/10.12989/mwt.2011.2.3.187

Modeling the electric transport of HCl and H_3PO_4 mixture through anion-exchange membranes

Stanisław Koter*, Monika Kultys and Barbara Gilewicz-Łukasik

Faculty of Chemistry, Nicolaus Copernicus University, 7 Gagarin St., 87-100 Toruń, Poland
(Received February 16, 2011, Accepted June 27, 2011)

Abstract. The electric transport of the mixture of hydrochloric and phosphoric acids through strong base (Neosepta ACM) and weak base (Selemion AAV) anion-exchange membranes was investigated. The instantaneous efficiency of HCl removal from the cathode solution, CE_{Cl}, with and without H_3PO_4 was determined. It was found that CE_{Cl} was 0.8-0.9 if the number of moles of elementary charge passed through the system, n_F, did not exceed ca. 80% of the initial number of HCl moles in the cathode solution, $n_{Cl,ca,0}$. The retention efficiency of H_3PO_4 in that range was close to one. The transport of acid mixtures was satisfactorily described by a model based on the extended Nernst-Planck and Donnan equations for n_F not exceeding $n_{Cl,ca,0}$. Among the tested model parameters, most important were: concentration of fixed charges, the porosity-tortuosity coefficient, and the partition coefficient of an undissociated form of H_3PO_4. For the both membranes, the obtained optimal values of fixed charge concentration, $\bar{c}_m$, were up to 40% lower than the literature values of $\bar{c}_m$ obtained from the equilibrium measurements. Regarding the H_3PO_4 equilibria, it was sufficient to consider H_3PO_4 as a monoprotic acid.

Keywords: anion-exchange membrane; hydrochloric acid; phosphoric acid; extended Nernst-Planck equation; current efficiency; electrodialysis

1. Introduction

One of the main applications of anion-exchange membranes (AMs) is the recovery of acids from spent industrial solutions using electrodialysis and diffusion dialysis (Scott 1995, Touaibia *et al.* 1996, Koter and Warszawski 2000, Nagarale *et al.* 2006, Luo *et al.* 2011). The papers describing the processes with AMs are numerous (Pourcelly *et al.* 1994, Lorrain *et al.* 1997, Cattoirs *et al.* 1999, Jörissen *et al.* 2003, Pisarska and Dylewski 2005, Melnyk and Goncharuk 2009, Banasiak and Schäfer 2009). However, papers focused on the theoretical aspects of the transport of acids in those processes are rather rare and mainly devoted to the concentration driven transport (Palatý and Žáková 2001, 2003, Nikonenko *et al.* 2003, Prado-Rubio *et al.*, 2010). The papers on the transport modeling are useful not only for the cognitive reasons, but also for the practical ones. A correct model enables simulating separation processes which can significantly reduce a number of expensive experiments needed to find the optimal process conditions.

This is a continuation of our work on the modeling of electric transport of acids through AMs. In the previous paper (Koter 2008), the possibility of sulfuric and acetic acids separation using anion-exchange membrane was investigated. In (Koter and Kultys 2008), the H_2SO_4 transport through strong-base and weak-base AMs was modeled using the extended Nernst-Planck and Donnan equations. In (Koter

* Corresponding author, Professor, E-mail: skoter@chem.uni.torun.pl

and Kultys 2010), the transport of H_2SO_4+H_3PO_4 mixture was described. It was found that in H_2SO_4 solutions the effective fixed charge concentration of AMs, $\bar{c}_m$, is ca. one order of magnitude lower than that obtained from the equilibrium experiments. In the presence of H_3PO_4, AMs lose their selectivity which is reflected by a significant decrease in $\bar{c}_m$. In pure H_3PO_4 solutions, $\bar{c}_m$ is nearly zero indicating that the membrane is practically unselective. It was found that, assuming the association equilibrium between $H_2PO_4^-$ and the fixed charges of AM, the simulation of changes in H_3PO_4 concentration during H_2SO_4+H_3PO_4 mixture electrodialysis was significantly improved.

In this work, the AMs performance in HCl+H_3PO_4 mixtures electrodialysis is investigated. The separation efficiency of HCl and H_3PO_4 is determined. The comparison of the membrane selectivity in acid mixtures with that in a pure HCl solution is given. The experimental data are fitted using the model described previously (Koter 2008, Koter and Kultys 2008, 2010). A series of different model assumptions is tested to find the best one. The fitted parameters taken into account are: effective charge concentration, porosity-tortuosity coefficient, partition coefficient of an undissociated H_3PO_4, association constant related to the equilibrium between $H_2PO_4^-$ and the fixed charges. H_3PO_4 is treated as a monoprotic acid. However, also the presence of $H_5P_2O_8^-$ anions is considered.

2. Theory

The system to be modeled is shown in Fig. 1. The cell is divided into three compartments by anion exchange (AM) and bipolar (BM) membranes. BM is placed between AM and the anode in order to avoid Cl^- oxidation. The cathodic and the middle compartments contain a mixture of HCl and H_3PO_4 solutions; in the anode compartment, a H_2SO_4 solution circulates. In the applied electric field, anions move through AM to the middle compartment. There, they are electrically neutralized by protons created inside BM, where water splitting takes place. The created OH^- anions are

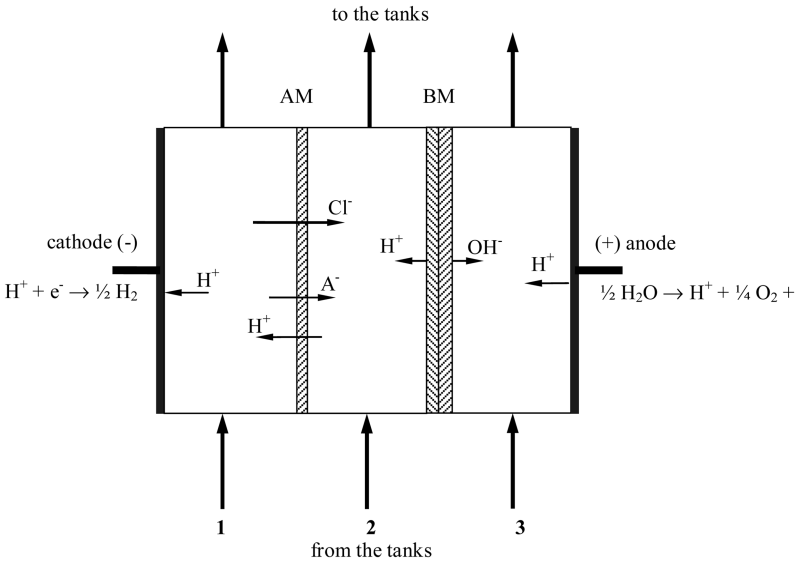

Fig. 1 Electric transport of ions in the system; A^- denotes $H_2PO_4^-$; for clarity, other anions coming from the H_3PO_4 dissociation are not shown.

neutralized by protons formed in the anode reaction. As the AM performance in strong acid solutions is not very good, it will be assumed that the efficiency of water splitting in BM is 100%.

Transport through AM and two adjacent concentration polarization layers (CPLs) is described by the extended Nernst-Planck equations (Eqs. (1,5) in (Koter 2008)

$$J_i=-D_i\left(\frac{dc_i}{dx}+z_ic_i\frac{d\varphi'}{dx}\right)+c_iJ_v \qquad \text{CPL}$$

$$J_i=k_{c,i}\left(-k_{DV\theta,i}D_i\left(\frac{dc_i}{dx}+z_ic_i\frac{d\varphi'}{dx}\right)+\alpha_ic_iJ_v\right) \qquad \text{membrane} \qquad (1a,b)$$

where

$$k_{c,i}\equiv\bar{c}_i/c_i, \quad k_{DV\theta,i}\equiv(V_p/\theta^2)(\bar{D}_i/D_i) \qquad (2), (3)$$

The flux of i-th species, J_i, and the volume flux, J_v, refer to the unit of membrane area. c_i, $k_{c,i}$ is the concentration, partition coefficient of the i-th species, respectively. $k_{DV\theta,i}$ is the porosity-tortuosity coefficient depending on the membrane porosity, V_p, tortuosity, θ, and the ratio of diffusion coefficients in the membrane, $\bar{D}_i$, and in the bulk solution, D_i. φ' is the dimensionless electric potential ($\varphi' = \varphi F/RT$). α_i is the convection coupling coefficient (Dresner 1972, Meares 1981, Peeters *et al.* 1998, Bowen and Welfoot 2002); $\alpha_i < 1$ for counterions and $\alpha_i > 1$ for coions. These inequalities result from the fact that in the charged pores, the concentration of coions is higher at the central part of a pore where the convection velocity is higher than average. At the same time, the concentration of counterions is higher in the vicinity of charged walls where the convection velocity is lower than average (Dresner 1972). In Eq. (1b) c_i and φ' refer to the hypothetical external solution being in equilibrium with the membrane pore solution at point x, where the concentration of the i-th species is $\bar{c}_i$. The equilibrium is expressed by the equality of ion electrochemical potentials which refer to the hypothetical solution and the membrane pore solution at a given membrane coordinate x

$$\tilde{\mu}_i(x)=\bar{\tilde{\mu}}_i(x) \qquad x\in\langle 0,l_m\rangle \qquad (4)$$

On the membrane boundaries ($x = 0$ and $x = l_m$) the hypothetical solution becomes the real one. As the work is focused on the modeling of ions electro-migration, in Eq. (1) the activity coefficient is neglected. This term is present only if there is a concentration gradient. At adequately high current density, the diffusion contribution to the total transport is small and the activity coefficient term can be neglected.

As the experiments are carried out under galvanostatic conditions, $d\varphi'/dx$ in Eq. (1) is replaced by the current density, j

$$j=F\sum_{i=1}^{n}z_iJ_i \qquad (5)$$

which yields the following transport equations

$$J_i=\frac{t_ij}{z_iF}+c_iJ_v-D_i\left(\frac{dc_i}{dx}-\frac{t_i}{z_iD_i}\sum_{j=1}^{3}D_jz_j\frac{dc_j}{dx}\right) \qquad \text{CPL}$$

$$J_i=k_{c,i}k_{DV\theta,i}\left(\frac{c_iz_iD_i}{b_1}\frac{j}{F}+\left(\frac{\alpha_i}{k_{DV\theta,i}}-D_iz_i\frac{b_2}{b_1}\right)c_iJ_v-D_i\left(\frac{dc_i}{dx}-\frac{c_iz_i}{b_1}\sum_j k_{c,j}k_{DV\theta,j}D_jz_j\frac{dc_j}{dx}\right)\right) \qquad \text{membrane} \qquad (6a,b)$$

In Eq. (6a), t_i is the transport number of i-th ion in a free solution

$$t_i = \frac{c_i z_i^2 D_i}{\sum_{j=1}^{3} D_j z_j^2 c_j} \tag{7}$$

In Eq. (6b), A_0 and A_1 are defined by

$$b_1 \equiv \sum_{j=1}^{3} D_j z_j^2 c_j k_{c,j} k_{DV,j}\,, \qquad b_2 \equiv \sum_{j=1}^{3} \alpha_j c_j z_j k_{c,j} \tag{8), (9}$$

In the investigated system only monovalent anions are taken into account: Cl^-, $H_2PO_4^-$, $H_5P_2O_8^-$. They are denoted by the indices 2, 3, 4, respectively; protons are denoted by 1, the undissociated H_3PO_4 – by 5. According to Eq. (4), assuming the activity coefficients ratio to be one, the concentrations of monovalent anions inside AM are given by

$$\overline{c}_i = c_i c_1 / \overline{c}_1 \qquad i = 2,\ 3,\ 4 \tag{10}$$

where $\overline{c}_1$ is the protons concentration inside AM. To obtain $\overline{c}_1$, Eq. (10) is substituted into the electroneutrality condition for AM which yields

$$\overline{c}_1 - \frac{c_1}{\overline{c}_i} \sum_{j=2}^{4} c_i + \overline{c}_m = 0 \tag{11}$$

where $\overline{c}_m$ is the concentration of positive fixed charges of AM. The sum of anion concentrations in Eq. (11) is equal to c_1. Thus, the solution of Eq. (11) is ($\overline{c}_1 > 0$)

$$\overline{c}_1 = \frac{1}{2}\left(\sqrt{\overline{c}_m^2 + 4c_1^2} - \overline{c}_m\right) \tag{12}$$

This solution is valid only for monovalent anions and anion-exchange membranes. The partition coefficient of anions, $k_{c,i}$, needed in Eq. (6), is calculated from Eqs. (12) and (10). The partition coefficient of undissociated H_3PO_4, $k_{c,5}$, is assumed as independent of concentration.

A number of the transported species is given by the ionic equilibria in the electrolyte solution. As the 2nd and 3rd dissociation constants of H_3PO_4, are low, the acid is treated as a monoprotic one

$$HA \leftrightarrow A^- + H^+ \qquad K_1 = 0.007121 \text{ (Leaist 1984)} \tag{13}$$

where HA denotes H_3PO_4, A^- – $H_2PO_4^-$. The additional reaction, which is considered here, is

$$HA + A^- \leftrightarrow HA_2^- \qquad K_0 = 1.3 \text{ (Leaist 1984)} \tag{14}$$

where HA_2^- denotes $H_5P_2O_8^-$. The molar concentrations of ions and neutral species in the solution are calculated using the equations

$$K_{0,c} = \frac{c_4 c^{\ominus}}{c_3 c_5}\,, \quad K_{1,c} = \frac{c_1 c_3}{c_5 c^{\ominus}} \tag{15a,b}$$

where $c^{\ominus}$ is the standard concentration ($c^{\ominus} = 1$ mol dm^{-3}), assuming that $K_{0,c}$ and $K_{1,c}$ are equal to the thermodynamic constants: $K_0 = 1.3$, $K_1 = 0.007121$. This simplification is justified by our results concerning the transport of H_2SO_4 through AMs (Tab. 4 in (Koter and Kultys 2008)). Taking the activity coefficients into account, the model fit of experimental data was practically the same. Only the optimal concentration of fixed charges was increased.

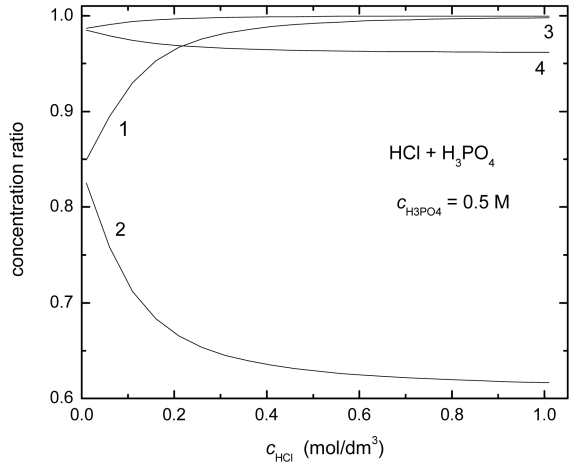

Fig. 2 Concentration ratio for different variants of ion equilibria in the aqueous HCl+H_3PO_4 mixture: 1 – $[H^+]_I/[H^+]_{II}$, 2 – $[A^-]_I/([A^-]+[HA_2^-])_{II}$, 3 – $[H^+]_{III}/[H^+]_{II}$, 2 – $([A^-]+[HA_2^-])_{III}/([A^-]+[HA_2^-])_{II}$ vs. c_{HCl} for c_{H3PO4} = 0.5 M;

Regarding the phosphoric acid equilibria, two variants will be examined here:
1) variant I with reaction (13) – species: H^+, $H_2PO_4^-$ and H_3PO_4,
2) variant II with reactions (13) and (14) – species: H^+, $H_2PO_4^-$, $H_5P_2O_8^-$ and H_3PO_4.
For the variant I, the protons concentration, c_1, is given by

$$c_1=\frac{1}{2}(c_2-K_1+((c_2+K_1)^2+4K_1c_A)^{1/2}) \tag{16}$$

For the variant II, c_1 is calculated by solving a cubic equation

$$(1-4K_0K_1)c_1^3+(4K_0K_1c_A-(1-8K_0K_1)c_2)c_1^2-K_1(c_A+K_0(c_A+2c_2)^2+K_1)c_1+K_1^2(c_A+c_2)=0 \tag{17}$$

Since c_1 has been found, the concentration of other ions is calculated from the equilibrium equations. The concentrations of ions in a free solution according to these variants are shown in Fig. 2. Here, the concentrations calculated assuming the equilibria (13), (14) and the reaction in which the dimer H_2A_2 ($H_6P_2O_8$) is created (Leaist 1984)

$$HA_2^- + H^+ \leftrightarrow H_2A_2 \tag{18}$$

are also shown. They are denoted as III. It can be seen that the difference is significant only for the variants I and II. As the concentrations of ions, especially of protons, calculated according to the variants II and III, are similar, it is justified to exclude the reaction (18) from the model. This is also supported by the fact that in the modeling of transport of H_2SO_4+H_3PO_4 mixtures through AMs (Koter and Kultys 2010) the reaction (18) had a negligible effect on the model simulations.

Similarly to our previous studies (Koter and Kultys 2010), the possibility of the fixed charges concentration reduction in the membrane by the association with the monovalent anion $H_2PO_4^-$ is also taken into account

$$-M^+ + H_2PO_4^- \leftrightarrow -MH_2PO_4 \tag{19}$$

This assumption is justified by the fact that in pure H_3PO_4 solutions the determined concentration

of the fixed charges is close to zero. It also substantially improves the model fitting of the H_2SO_4+H_3PO_4 data (Koter and Kultys 2010). The equilibrium constant of (19) is given by

$$K_{as,c}=\frac{(\overline{c}_{m,\max}-\overline{c}_m)c^{\ominus}}{\overline{c}_m\overline{c}_3} \tag{20}$$

from which the following expression for $\overline{c}_m$ results in

$$\overline{c}_m=\frac{\overline{c}_{m,\max}}{1+\overline{c}_3K_{as,c}/c^{\ominus}} \tag{21}$$

where $\overline{c}_{m,\max}$ is the maximal concentration of the fixed charges. After substituting Eq. (21) into (11), for both variants, the cubic equation is obtained

$$\overline{c}_1^3+(\overline{c}_{m,\max}+c_1c_3K_{as})\overline{c}_1^2-c_1^2\overline{c}_1-c_1^3c_3K_{as}=0 \tag{22}$$

which has to be solved with respect to $\overline{c}_1$.

The total fluxes of HCl, J_2, and of H_3PO_4 through AM

$$J_A\equiv J_3+J_4 \qquad \text{(variant I)}$$

$$J_A\equiv J_3+J_4+2J_5 \qquad \text{(variant II)} \tag{23a,b}$$

are calculated under the assumption that they are the same in both CPLs and the membrane. The solving method is described in (Koter 2008, Koter and Kultys 2008, 2010). The following values of the diffusion coefficient, D_i, are assumed in the calculations: $H^+ - 9.31\times10^{-9}$, $Cl^- - 2.03\times10^{-9}$ (Robinson and Stokes 1959), $H_2PO_4^- - 0.879\times10^{-9}$, $H_3PO_4 - 0.87\times10^{-9}$, $H_5P_2O_8^- - 0.8\times10^{-9}$ m^2s^{-1} (Leaist 1984) ($T = 298$ K). The above mentioned values of ion diffusivities refer to the infinity dilution. The method of the volume flow, J_v, calculation from the experimental data is described in the Appendix. The thickness of the polarization layer, $l_{pol} = 49$ μm, for the membrane module used in this work was determined previously from the current-voltage curves (Koter and Kultys 2008).

3. Experimental

The membrane electrodialysis of both the HCl+H_3PO_4 mixture and HCl solutions was performed by the batch method using the membrane cell (FuMA-Tech GmbH) and the setup shown in Fig. 3. The cell was divided into three compartments by an anion exchange membrane and a bipolar one (BP1, Tokuyama Co., Japan) in order to avoid Cl^- oxidation at the anode. Independent experiments involving only BP1 proved that the diffusion and electric transports of acids through BP1 were negligible compared to that through the tested anion-exchange membranes: the Neosepta ACM (Tokuyama Co., Japan) and the Selemion AAV (Asahi Glass Engineering Co., Japan). The thickness values of ACM and AAV, obtained with a thickness gauge, were 0.12, 0.1 mm, respectively. The active area of the membrane in the module was 3.5×14 $cm^2 = 49$ cm^2. The solutions were circulated using the ASTI pumps. In all the experiments, the volumetric flow of the cathode solution was 1.3, of the anode solution – 1.1 dm^3/min. Electric current was supplied by the Sorensen DCR 300-9B2 power supply. The acid diffusion experiments (D) were all conducted in the same setup. The parameters of the experiments are gathered in Table 1. The concentration and volume values are the approximated ones. The exact values could deviate from the tabulated values by ca. 5%. The acids

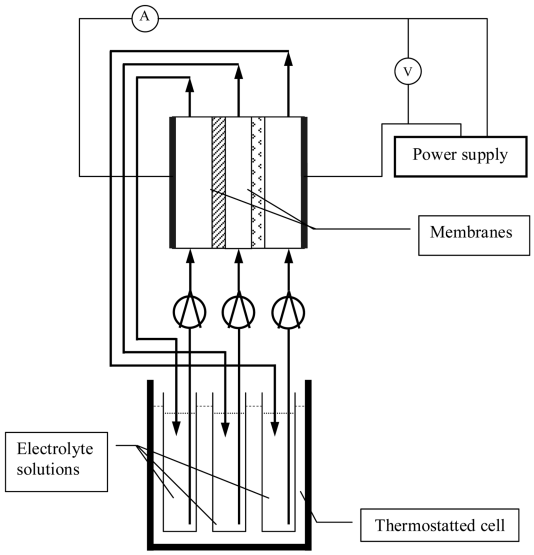

Fig. 3 Experimental setup

Table 1 Parameters of experiments: j – current density, $c_A - H_3PO_4$ concentration, $c_{ca,0}$, $c_{an,0}$ – the initial concentrations of acids in the cathode, anode compartment, respectively; the volumes of solutions: $V_{ca,0} = V_{an,0} = 0.3$ dm^3

exper.	j [mA cm^{-2}]	$c_{HCl,ca,0}$ [M]	$c_{A,ca,0}$ [M]	$c_{HCl,an,0}$ [M]	$c_{A,an,0}$ [M]
E1	100	1	0.53	0.1	<0.002
E2	50	1	0.53	0.1	<0.002
E3	100	2	0.53	0.1	<0.002
E4	50	2	0.53	0.1	<0.002
D	0	2	0.5	<0.01	<0.002

concentration was determined by the pH-metric titration (Radiometer) of samples (0.3–1 ml) taken during the process. The mass of the solutions was measured before and after the experiment. The mass fluxes through the membranes were calculated from the formulas derived in the Appendix.

3.1 Calculations

A block diagram of model calculations is shown in Fig. 4. The input parameters were: masses and concentrations of solutions at $t = 0$ ($m_{\alpha,0}$, $m'_{\beta,\alpha,0}$), current density, j, membrane area, S_m, and the model parameters. In the time loop, the ion fluxes through AM, masses, and concentrations of the cathode and middle solutions were calculated. The mass changes due to sampling ($m_{\alpha,t} = m_{\alpha,t} - m_{sam,\alpha,is}$) were also taken into account. The time step, Δt, was set to be 80 s. It was checked that this value gives practically the same results of the process simulation as the smaller step values do. Each polarization layer was divided into 3 slices, the membrane – into 20 slices. The further increase in the number of slices did not change the results. The thickness values of the membrane slices were not the same; the slices were thinner in the regions of high concentration gradient. The optimal

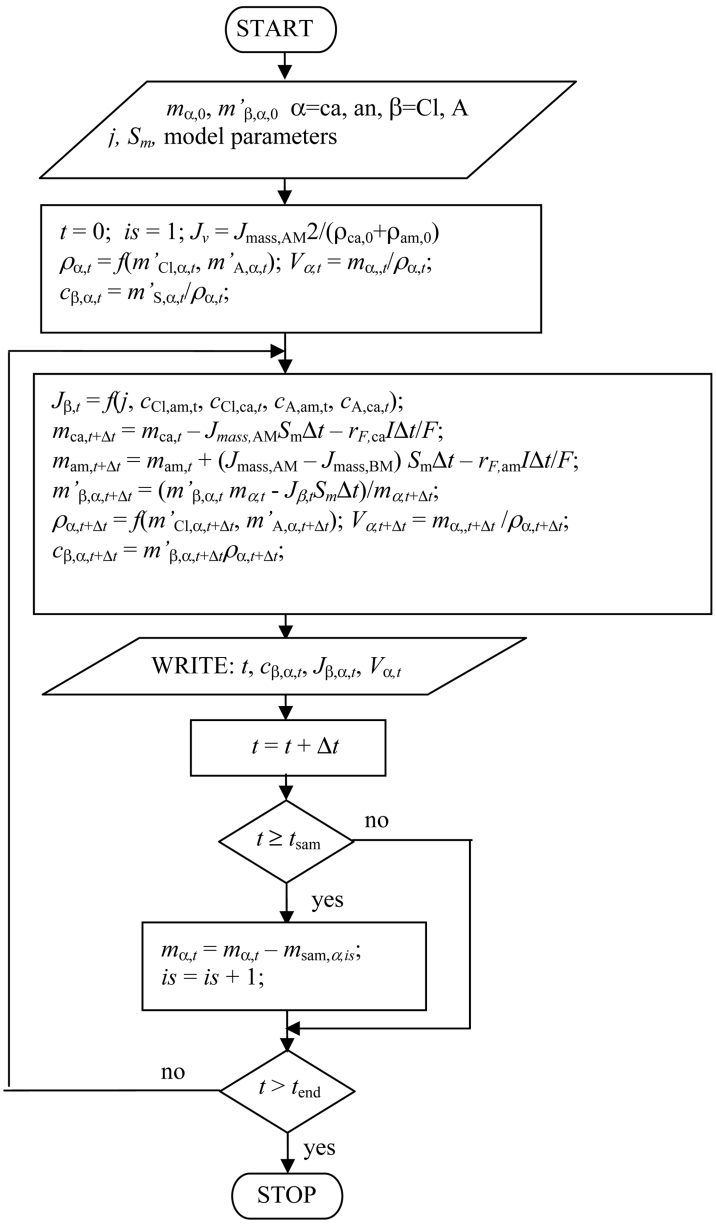

Fig. 4. Block diagram of model calculations

values of the fitted parameters were found by minimizing the sum of squared residuals of acid concentrations. The minimizing procedure was based on the observation that the fitting of diffusion data depends predominantly on the parameters $k_{DV\theta,i}$ and $k_{c,5}$, whereas the fit of electrodialysis data – on $\overline{c}_m$ and $k_{c,5}$. Thus, the optimal values of parameters were found by repeatedly fitting the electrodialysis and diffusion data using the simplex method. Because the flows of solutions passing the module compartments were the same as in our previous studies (Koter and Kultys 2008), the same thickness value of the polarization layer, $l_{pol} = 49$ μm, was assumed.

4. Results and discussion

One of the main aims of this work was to find whether the presented model is able to fit satisfactorily the experimental results of HCl+H_3PO_4 transport through AMs. The unknown model parameters included: α_i, $k_{DV\theta,i}$, $k_{c,5}$, $\overline{c}_m$ (no association assumption) or $K_{as,c}$ and $\overline{c}_{m,\max}$ (association). Many different model assumptions were examined. It was found that the convection coupling coefficient, α_i, insignificantly improved the data fit in comparison to other parameters. Contrary to the H_2SO_4+H_3PO_4 mixture transport (Koter and Kultys, 2010), the association assumption given by Eq. (19) did not prove useful for the HCl+H_3PO_4 mixture. The other model assumptions, i.e. $k_{DV\theta}$ common for all the transported species with $k_{c,5} = 1$ and the presence of $H_5P_2O_8^-$ anions, did not improve the model fitting. Thus, only two cases of the variant I (H_3PO_4 as a monoprotic acid) are presented here:

I-1: $k_{c,5} = 1$, fitted parameters: $\overline{c}_m$, $k_{DV\theta,\mathrm{Cl}}$ and $k_{DV\theta,\mathrm{A}}$,

I-2: fitted parameters: $\overline{c}_m$, $k_{DV\theta}$ and $k_{c,5}$,

where $k_{DV\theta} \equiv k_{DV\theta,1} = k_{DV\theta,2} = k_{DV\theta,3} = k_{DV\theta,4} = k_{DV\theta,5}$, $k_{DV\theta,Cl} \equiv k_{DV\theta,1} = k_{DV\theta,2}$, $k_{DV\theta,\mathrm{A}} \equiv k_{DV\theta,3} = k_{DV\theta,4} = k_{DV\theta,5}$.

4.1 Diffusion

The acid concentration ratio of dilute solution to the initial concentrate versus time in the diffusion experiment is shown in Fig. 5(a),(b). The lines present the model fitting. The values of fitted parameters are shown in Table 4. As it was mentioned in the experimental part, the fit of the diffusion data is sensitive to the values of $k_{DV\theta,i}$ and $k_{c,5}$ coefficients. Therefore, these data were used to obtain the optimal values of $k_{DV\theta,i}$ and $k_{c,5}$. It was found that the both considered cases I-1 and I-2 easily fit the diffusion data.

The mean diffusion permeabilities of the acids calculated according to Eq. (5a) in the Appendix are shown in Table 2. It can be seen that ACM shows more than two times higher permeability of the both acids when compared to AAV. As the thickness of ACM is 20% higher than that of AAV,

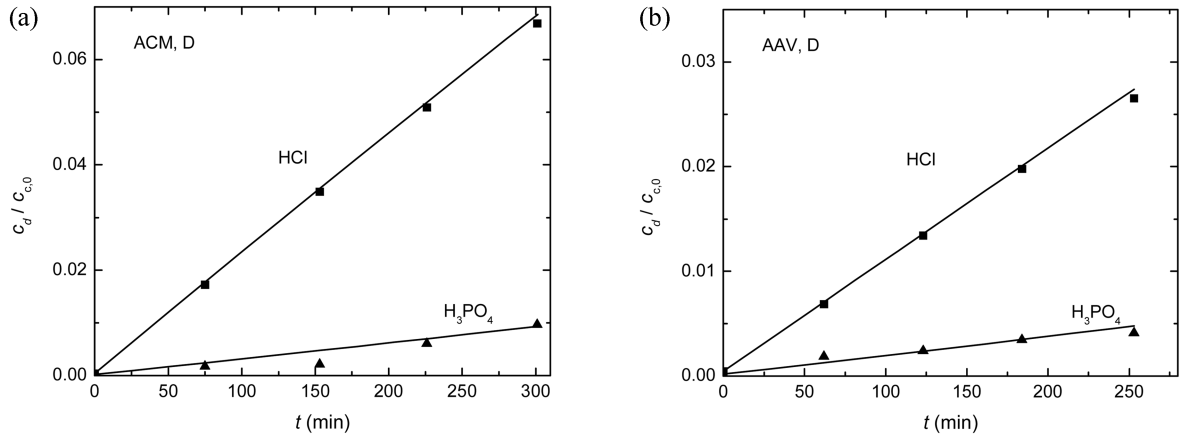

Fig. 5 $c_d/c_{c,0}$ in the diffusion experiment with the mixture HCl+H_3PO_4; a) ACM, b) AAV; line – model fit, optimal values of fitted parameters are in Table 4.

Table 2 Mean diffusion permeability of acids $\langle P_{s,i} \rangle$ [10^{-7} m/s] calculated from Eq. (A5a) for the HCl+H_3PO_4 mixture

acid	ACM	AAV
H_3PO_4	0.31	0.15
HCl	2.3	1.0

the discrepancy of $\langle P_{s,i} \rangle l_m$ characterizing the membrane material is even larger. A similar discrepancy was observed for the H_2SO_4+H_3PO_4 mixtures (Koter and Kultys 2010). Comparing the acid permeabilities, $\langle P_{s,A} \rangle$ (H_3PO_4) is ca. 7 times lower than $\langle P_{s,Cl} \rangle$ (HCl), although for aqueous solutions D_{HCl} is ca. 3.5 times higher than D_{H3PO4} (for 0.5 M solution $D_{HCl} = 3.18\times10^{-9}$ m^2s^{-1} (Robinson and Stokes 1959), $D_{H3PO4} = 0.85\times10^{-9}$ m^2s^{-1} (Edwards and Huffman 1959)). In aqueous solutions ($c >$ 0.1 M), the dominant diffusing form is undissociated H_3PO_4, as in the permeation of H_3PO_4 through AMs in the presence of HCl. Thus, since the ratio $\langle P_{s,A} \rangle / \langle P_{s,Cl} \rangle \approx 0.14$ is significantly lower than $D_{H3PO4}/D_{HCl} \approx 0.3$, it can be concluded that either the diffusivity of H_3PO_4 in the membrane is more reduced comparing to the mobility of Cl^- anions or the partition coefficient of undissociated H_3PO_4, $k_{c,5}$, is below 1. For strong acids which diffuse in the dissociated form, the ratio $\langle P_{s,H2SO4} \rangle / \langle P_{s,Cl} \rangle \approx 0.8$ is much closer to $D_{H2SO4}/D_{HCl} \approx 0.67$ ($D_{H2SO4} = 2.13\times10^{-9}$ m^2/s in 1 M solution at 25°C (Leaist 1984b).

4.2 Electric transport

Before electric transport of ions is discussed, a comment on the mass flow should be made. It can be seen (Table 3) that the electroosmotic mass flow (E1-E4) is much higher than the osmotic one (D). Thus, the osmotic part of that flow is very low and the main part is the electroosmotic flow of water induced by the migration of ions. The values of transported mass divided by the number of moles of passed elementary charge, $FJ_{mass,A}/j$, are similar for the both membranes and for the both current density values (E1, E3 – $j = 1000$, E2, E4 – $j = 500$ A/m^2).

The comparison of H_3PO_4 fit in various cases of the model assumptions is shown in Fig. 6. It is satisfactory only in the case I-2 where the partition coefficient of undissociated H_3PO_4, $k_{c,5}$, is chosen

Table 3 Mass flow through the anion-exchange membranes

exper.	$J_{mass,AM}$ [g $m^{-2}s^{-1}$]	$FJ_{mass,AM}/j$ [g mol^{-1}]
	ACM	
E1	0.67	65
E2	0.34	65
E3	0.62	60
E4	0.35	67
D	0.009	
	AAV	
E1	0.69	67
E2	0.35	67
E3	0.67	65
E4	0.37	70
D	–0.014	

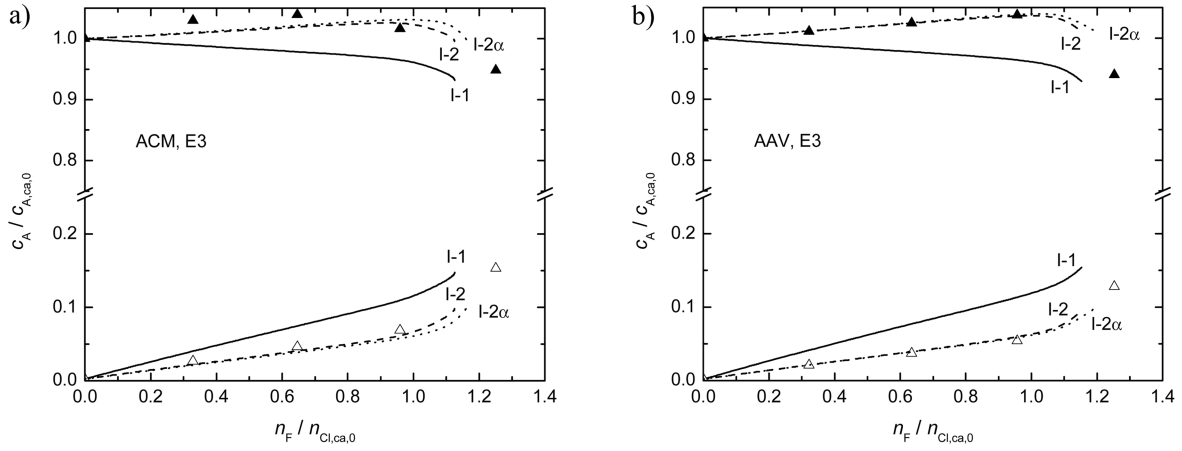

Fig. 6 Comparison of different model assumptions on the H_3PO_4 fit of experimental data for ACM (a) and AAV (b), experiment E3.

Table 4 Optimal model parameters $\bar{c}_m$ and $k_{DV\theta,i}$ for ACM and AAV in contact with the HCl+H_3PO_4 mixtures for the model cases I-1 and I-2

exper.	I-1, I-2 $\bar{c}_m$ [M]		I-1				I-2			
			ACM		AAV		ACM		AAV	
	ACM	AAV	$k_{DV\theta,Cl}$	$k_{DV\theta,A}$	$k_{DV\theta,Cl}$	$k_{DV\theta,A}$	$k_{DV\theta}$	$k_{c,5}$	$k_{DV\theta}$	$k_{c,5}$
D	3	3	0.008	0.0035	0.0033	0.0027	0.008	0.48	0.0033	0.78
	4	3.6	0.0087	0.0035	0.0035	0.0028	0.0087	0.46	0.0035	0.74
E1	3	3	0.008	0.001[a)]	0.0033	≤0.002	0.008	0.48	0.0033	0.6
E2	3	3.6	0.008	0.001[a)]	0.0035	→0[b)]	0.008	0.48	0.0035	0.46
E3	4	3.6	0.0087	→0[b)]	0.0035	→0[b)]	0.0087	0.48	0.0035	0.46
E4	4	3.6	0.0087	→0[b)]	0.0035	→0[b)]	0.0087	0.48	0.0035	0.46

[a)] The fit of H_3PO_4 is acceptable, however further decrease in $k_{DV\theta,A}$ will not improve the fit.
[b)] It could not be fitted by decreasing $k_{DV\theta,A}$.

as the fitted parameter. Its optimal value is ca. 0.5 (Table 4), whereas it was not possible to fit the H_3PO_4 data with $k_{DV\theta,A}$ going even to zero. In Fig. 6, also the case I-2 with the ion convection coefficients, α_i, higher than 1 for coion H^+ and lower than 1 for counterions ($\alpha_1 = 1.5$, $\alpha_2 = \alpha_3 = 0.5$, $\alpha_5 = 1$) is shown (denoted as I-2α, dotted line). It is seen that for this assumption, the simulation of the process in the whole range of n_F is not possible. For HCl, all these cases yielded a similar data fit.

The optimal values of $\bar{c}_m$ for ACM (Table 4) are: 3 M for the experiments E1, E2, and 4 M – for E3 and E4 where the initial HCl concentration is higher than that in E1, E2. For AAV $\bar{c}_m$ is 3.6 M for E2, E3, E4, and 3 M – for E1. As there are two optimal values of $\bar{c}_m$, the parameters $k_{DV\theta,i}$ and $k_{c,5}$ were optimized using these two values and the diffusion data. However, it was not possible to fit the H_3PO_4 concentration changes in the E experiments using $k_{DV\theta,A}$. It could be done only by fitting $k_{c,5}$. In the case of the AAV membrane, the values of $k_{c,5}$ should be lower than those resulting from the D experiment (D: $k_{c,5} = 0.74$-0.78, E: $k_{c,5} = 0.46$-0.6). For the both membranes $k_{c,5}$ has

similar optimal values.

The optimal values of $\bar{c}_m$ for $HCl+H_3PO_4$ mixtures (Table 4) are close to those obtained for pure HCl solutions ($\bar{c}_m$ = ca. 3.8 M for both membranes). It means that the presence of H_3PO_4 has no influence on the effective fixed charge concentration, contrary to the $H_2SO_4+H_3PO_4$ mixtures at similar acid concentrations (Koter and Kultys 2010). It should be also noted that the obtained $\bar{c}_m$ is lower than that resulting from the equilibrium measurements. According to (Pourcelly *et al*. 1994), the values of ion-exchange capacity of ACM and AAV are 1.01 and 0.95 mequiv. per gram of dried membrane, respectively, whereas those of swelling are 10.2 (ACM) and 11.1 (AAV) moles of H_2O per mole of exchanging site in 0.1 M H_2SO_4. Thus, the concentration of the fixed charges in moles per kg of water is 5.5 (ACM) and 4.8 (AAV).

The concentration changes for all the experiments are shown in Figs. 7 and 8. Only the lines of

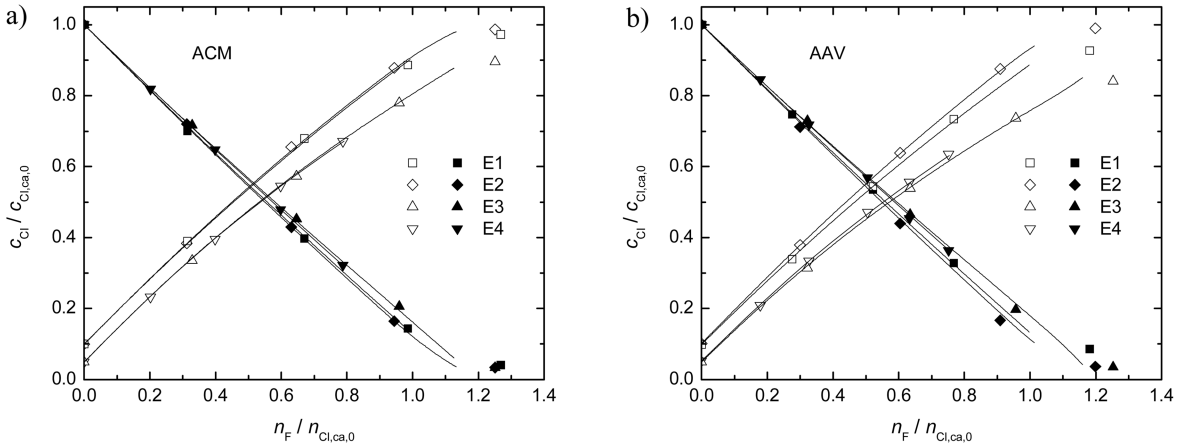

Fig. 7 Ratio $c_{Cl}/c_{Cl,ca,0}$ for the cathode and anode solutions vs. $n_F/n_{Cl,ca,0}$ for ACM (a) and AAV (b); symbols – experiment (Table 1); lines – model fit I-2 (Table 4).

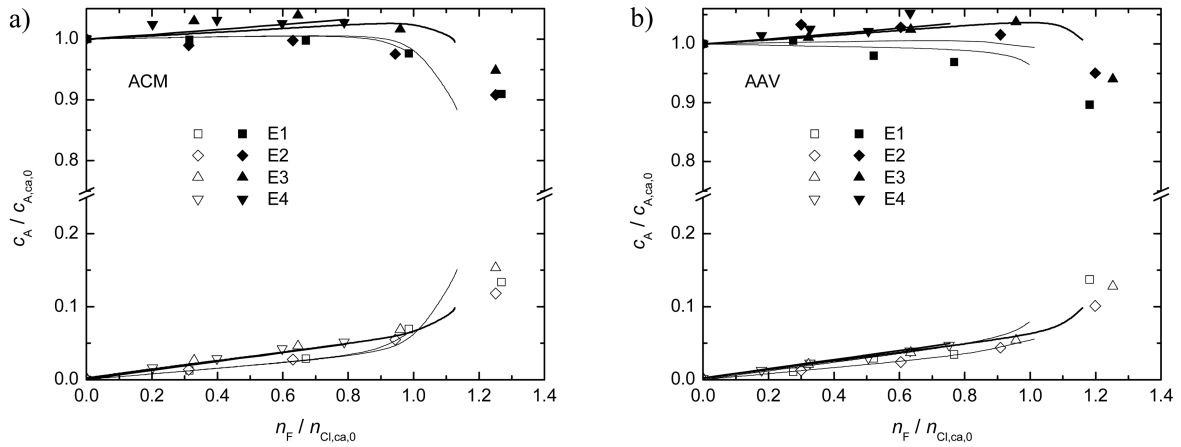

Fig. 8 Ratio $c_A/c_{A,ca,0}$ for the cathode and anode solutions vs. $n_F/n_{Cl,ca,0}$ for ACM (a) and AAV (b); symbols – experiment (Table 1); lines – model fit I-2 (Table 4).

the model fit I-2 are shown. It is seen that for $n_F/n_{Cl,ca,0}$ lower than ca. 0.9, the decrease and increase in HCl concentrations are almost linear. In that range of $n_F/n_{Cl,ca,0}$, the concentration of H_3PO_4 in the cathode solution is almost constant, although its concentration in the middle compartment increases. It is caused by the electroosmotic flow of water dragged by anions through AM to the middle compartment. Thus, the decreasing volume of the cathode solution keeps the H_3PO_4 concentration on the same level. For $n_F/n_{Cl,ca,0}$ higher than ca. 0.9, a significant increase in H_3PO_4 concentration is observed. It is caused by a substantial decrease in HCl concentration which increases the H_3PO_4 dissociation. Consequently, the migration of $H_2PO_4^-$ anions through the membrane increases.

Using the concentration dependencies on n_F (Fig. 7, Fig. 8), current efficiency of HCl removal from the cathode solution, CE_{Cl}, and the current efficiency of H_3PO_4 retention, $CE_{ret,A}$, in that solution were calculated. CE_{Cl} was calculated from the formula

$$CE_{Cl} \equiv -V_{ca,0}\frac{dc_{Cl,ca}}{dn_F} = -\frac{dc_{Cl,ca}/c_{Cl,ca,0}}{dn_F/n_{Cl,ca,0}} \tag{24}$$

where $V_{ca,0}$ is the initial volume of the cathode solution, n_F is the number of moles of the elementary charge passed through the system. For comparison, we also calculated *CE* based on the change of a number of moles of a given species in the cathode solution

$$CE_{n,\alpha} \equiv -\frac{dn_{\alpha,ca}}{dn_F} = -V_{ca}\frac{dc_{\alpha,ca}}{dn_F} - c_{\alpha,ca}\frac{dV_{ca}}{dn_F} \qquad \alpha = \text{Cl, A} \tag{25}$$

The choice of the *CE* definition depends on the preferences. Eq. (24) reflects only the concentration change. If there is no change, $CE = 0$. The advantage of such a *CE* means there is no need to measure the volume changes during the process. Eq. (25) yields $CE > 0$ even if the concentration change is zero. However, it better characterizes the membrane transport of ions. For the poorly dissociated H_3PO_4 being in the mixture with a strong acid, the efficiency of retention, $CE_{ret,A}$, defined by

$$CE_{ret,A} \equiv 1 - CE_A = 1 - \frac{dc_{A,ca}/c_{A,ca,0}}{dn_F/n_{A,ca,0}} \tag{26}$$

or by

$$CE_{ret,n,A} \equiv 1 - CE_{n,A} \tag{27}$$

is more appropriate, where $CE_{n,A}$ is given by Eq. (25). To calculate *CE*, the acid concentration should be expressed as a function of n_F, $c(n_F)$. As the best model fit did not cover the whole range of n_F, the model function $c(n_F)$ was joined with a cubic equation ($c = a_0 + a_1 n_F + a_2 n_F^2 + a_3 n_F^3$). In the joint point, the first and second derivatives of the cubic equation were set to be equal to the derivatives of the model function. Using these conditions and minimizing the deviation of c from the experimental values of c, the coefficients of the cubic equation, a_i, were found.

The comparison of *CE* to CE_n is shown in Fig. 9. It is seen that in the case of HCl removal, at the beginning of the experiment $CE_{n,Cl} > CE_{Cl}$, at the end – the relation is reversed. In the case of H_3PO_4 retention, $CE_{ret,n,A}$ is slightly lower than $CE_{ret,A}$ in the whole range of n_F because the volume of the cathode solution decreases during the process. As the differences in the values of *CE* and CE_n are not so important, and *CE* can be easily determined, only *CE* based on the concentration changes will be discussed further in the text.

In Fig. 10, the efficiency of HCl removal, CE_{Cl}, is shown. It is seen that CE_{Cl} for the both membranes (ACM and AAV) is similar, *i.e.* for $n_F/n_{Cl,ca,0} \leq 0.8$-0.9 CE_{Cl} is above 0.8, and then it strongly decreases.

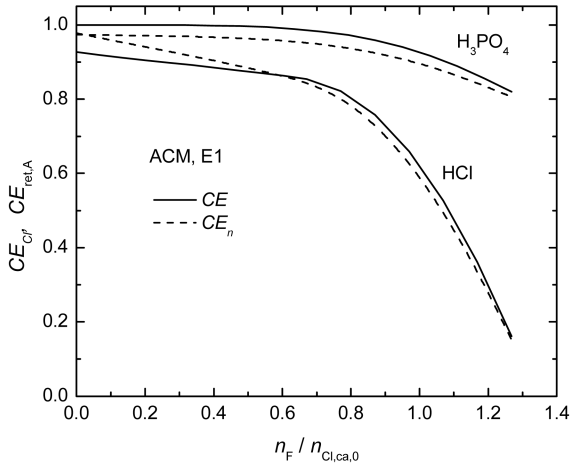

Fig. 9 Comparison of CE_{Cl} (Eq. (24) and $CE_{ret,A}$ (25) with $CE_{n,Cl}$ (Eq. (26)) and $CE_{ret,n,A}$ (Eq. (27)) for ACM, E1.

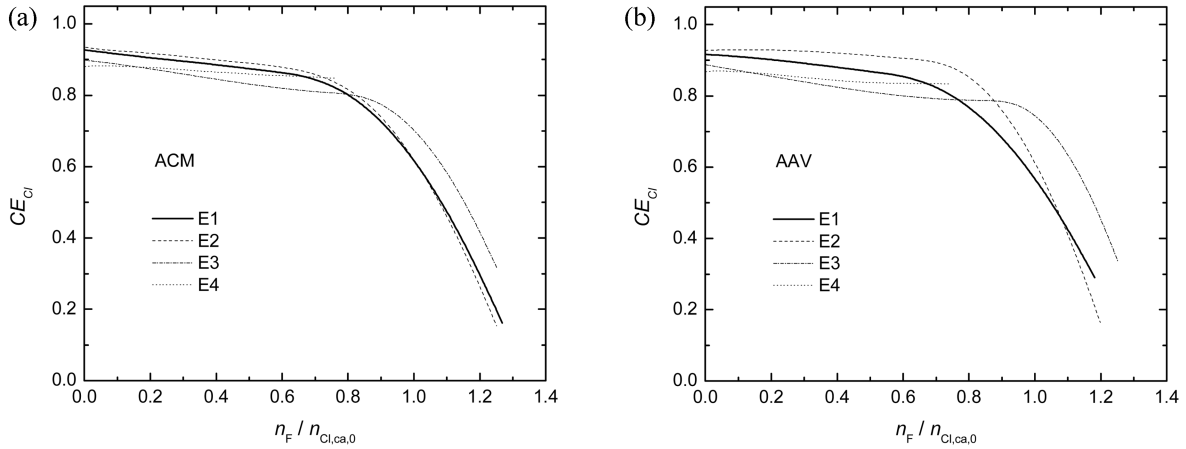

Fig. 10 Instantaneous current efficiency of HCl removal, CE_{Cl} (Eq.(24)); conditions of experiments are in Table 1; (a) ACM, (b) AAV.

These changes are correlated with the changes of H_3PO_4 retention efficiency, $CE_{ret,A}$, which is nearly one, and for $n_F/n_{Cl,ca,0} > 0.8$ it also strongly decreases (Fig. 11). The differences between CE for the experiments E1-E4 are small if $n_F/n_{Cl,ca,0} \leq 0.8$. In the E3 and E4 experiments in which higher HCl concentration was used, CE_{Cl} is slightly lower than that in E1 and E2 because of higher Donnan sorption of HCl. The current density (500, 1000 A/m^2) has no significant effect on CE. At the end of the process ($n_F/n_{Cl,ca,0} > 0$), CE_{Cl} is higher for the experiments with higher initial HCl concentrations. The reason is that at the same value of $n_F/n_{Cl,ca,0}$ the HCl concentrations in E3 and E4 are higher than those in E1 and E2. Thus, the transport of $H_2PO_4^-$ anions lowering CE_{Cl} is still diminished.

In Fig. 12, the comparison of CE_{Cl} with that obtained for pure HCl solutions is shown. It is seen that in the experiment E3 ($c_{HCl,ca,0}/c_{A,ca,0} \approx 4$), CE_{Cl} is similar to that obtained for pure HCl solutions (for $n_F/n_{Cl,ca,0} <$ ca. 0.8). In the experiment E1, CE_{Cl} is smaller than that for HCl solutions because of

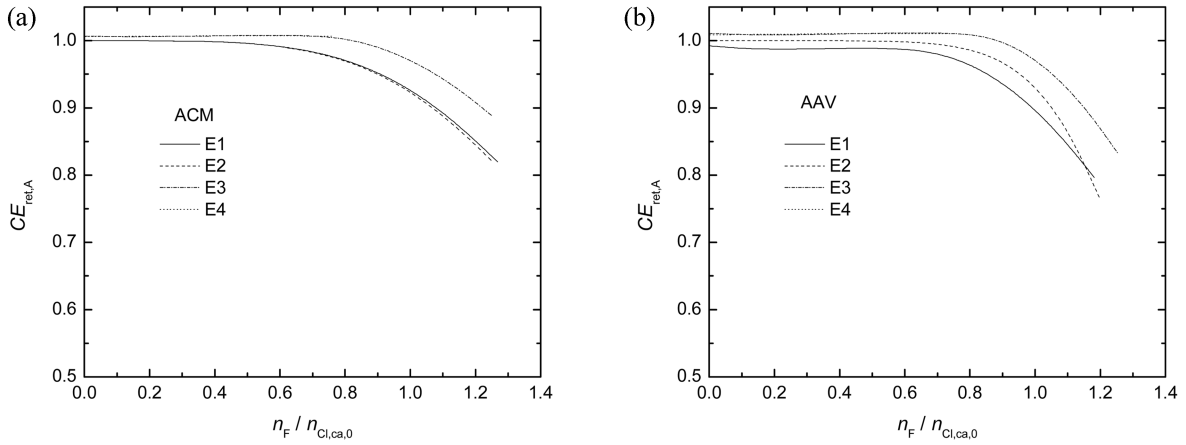

Fig. 11 Instantaneous current efficiency of H_3PO_4 retention, $CE_{ret,A}$ (Eq. (26)); conditions of experiments are in Table 1; (a) ACM, (b) AAV.

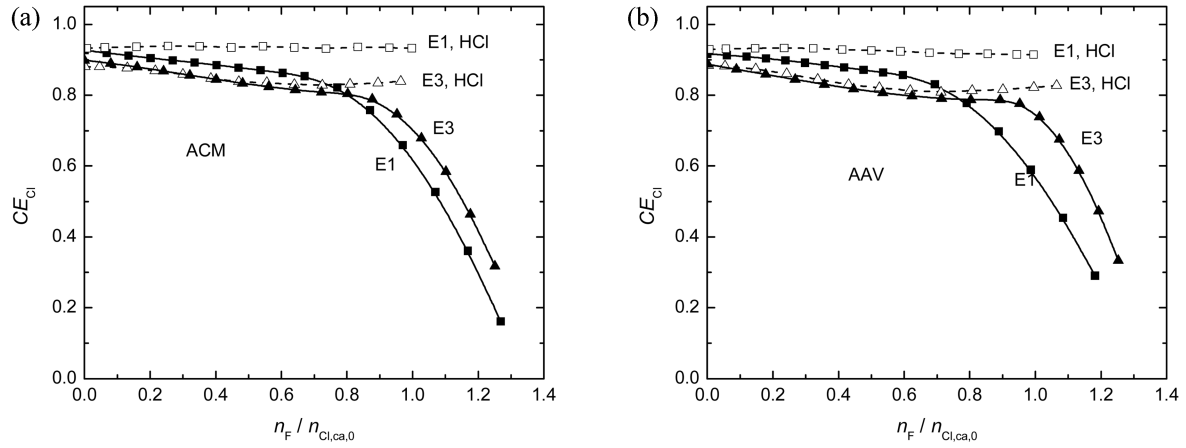

Fig. 12 Comparison of CE_{Cl} (Eq. (24)) for single HCl solutions and for HCl+H_3PO_4 mixtures; conditions of experiments are in Table 1; (a) ACM, (b) AAV.

a lower $c_{HCl,ca,0}/c_{A,ca,0}$ ratio (≈ 2). In comparison to the H_2SO_4+H_3PO_4 mixtures, the efficiency of HCl removal is significantly higher. For example, for $n_F/n_{Cl,ca,0} = 1$, $c_{Cl,ca}/c_{Cl,ca,0}$ reaches 0.1 (Fig. 7), whereas for H_2SO_4, $c_{S,ca}/c_{S,ca,0}$ is merely ca. 0.5 (Fig. 4 in (Koter and Kultys 2010)). The H_3PO_4 retention is also higher in the case of HCl+H_3PO_4 mixtures.

5. Conclusions

The HCl removal from the mixture of HCl+H_3PO_4, CE_{Cl}, and the H_3PO_4 retention efficiency, $CE_{ret,A}$, by means of the anion-exchange membranes ACM and AAV are efficient if the number of moles of the elementary charge passed through the system, n_F, does not exceed ca. 80% of the initial number of HCl moles in the mixture, $n_{Cl,ca,0}$. In that range of $n_F/n_{Cl,ca,0}$, CE_{Cl} (= 0.8-0.9) is close to that

obtained for pure HCl solutions. $CE_{ret,A}$ is close to one. Both of the investigated membranes, ACM and AAV, show similar characteristics.

The transport model based on the extended Nernst-Planck equation and the Donnan equilibrium satisfactorily describes the electric transport of $HCl+H_3PO_4$ mixture through anion-exchange membranes for n_F not exceeding $n_{Cl,ca,0}$. Among the tested model parameters the most important are: the concentration of the fixed charges, $\bar{c}_m$, the porosity-tortuosity coefficient, $k_{DV\theta}$, and the partition coefficient of the undissociated form of H_3PO_4, $k_{c,5}$. The optimal values of $\bar{c}_m$ for the both membranes are up to 40% lower than those obtained from the equilibrium experiments. The porosity-tortuosity coefficient, $k_{DV\theta}$, for ACM is more than two times higher than that for AAV. It indicates that the pores of AAV are narrower and/or more tortuous than those of ACM. When compared to $H_2SO_4+H_3PO_4$ mixtures, the assumption on association equilibrium between $H_2PO_4^-$ and the membrane fixed charges or additional H_3PO_4 equilibria does not improve the fitting of $HCl+H_3PO_4$ data.

Acknowledgement

The authors thank Eurodia Industrie S.A. and Asahi Glass Engineering Co. for supplying the samples of membranes (ACM, AAV, respectively).

References

Banasiak, L.J. and Schäfer, A.I. (2009), "Removal of boron, fluoride and nitrate by electrodialysis in the presence of organic matter", *J. Membrane Sci.*, **334**(1-2), 101-109.

Bowen, W.R. and Welfoot, J.S. (2002), "Modelling the performance of membrane nanofiltration—critical assessment and model development", *Chem. Eng. Sci.*, **57**(7), 1121-1137.

Brandt, S. (1976), *Metody statystyczne i obliczeniowe analizy danych*, PWN, Warszawa.

Cattoirs, S., Smets, D. and Rahier, A. (1999), "The use of electro-electrodialysis for the removal of sulphuric acid from decontamination effluents", *Desalination*, **121**(2), 123-130.

Dresner, L. (1972), "Stability of the extended Nernst-Planck equations in the description of hyperfiltration through ion-exchange membranes", *J. Phys. Chem.*, **76**(16), 2256-2267.

Edwards, O.W. and Huffman, E.O. (1959), "Diffusion of aqueous solutions of phosphoric acid at 25º", *J. Phys. Chem.*, **63**(11), 1830-1833.

Jörissen, J., Breiter, S.M. and Funk, C. (2003), "Ion transport in anion exchange membranes in presence of multivalent anions like sulfate or phosphate", *J. Membrane Sci.*, **213**(1-2), 247-261.

Koter, S. and Warszawski, A. (2000), "Electromembrane processes in environment protection", *Polish J. Environ. Studies*, **1**, 45-56.

Koter, S. (2008), "Separation of weak and strong acids by electro-electrodialysis - experiment and theory", *Sep. Purif. Technol.*, **60**(3), 251-258.

Koter, S. and Kultys, M. (2008), "Electric transport of sulfuric acid through anion-exchange membranes in aqueous solutions", *J. Membrane Sci.*, **318**(1-2), 467-476.

Koter, S. and Kultys, M. (2010), "Modeling the electric transport of sulfuric and phosphoric acids through anion-exchange membranes", *Separation and Purification Technology*, **73**(2), 219-229.

Leaist, D.G. (1984a), Diffusion in Dilute Aqueous Solutions of Phosphoric Acid, *J. Chem. Soc*., *Faraday Trans. I*, **80**, 3041-3050.

Leaist, D.G. (1984b), "Diffusion in aqueous solutions of sulfuric acid", *Can. J. Chem.*, **62**, 1692-1697.

Lorrain, Y., Pourcelly, G. and Gavach, C. (1997), "Transport mechanism of sulfuric acid through an anion exchange membrane", *Desalination*, **109**(3), 231-239.

Luo, J., Wu, C., Xu, T. and Wua, Y. (2011), "Diffusion dialysis-concept, principle and applications", *J. Membrane*

Sci., **366**(1-2), 1–16.
Meares, P. (1981), "Coupling of ion and water fluxes in synthetic membranes", *J. Membrane Sci.*, **8**(3), 295-307.
Melnyk, L. and Goncharuk, V. (2009), Electrodialysis of solutions containing Mn (II) ions, *Desalination*, **241**(1-3), 49-56.
Nagarale, R.K., Gohil, G.S. and Shahi, V.K. (2006), "Recent developments on ion-exchange membranes and electro-membrane processes", *Adv. Colloid Interf. Sci.*, **119**(2-3), 97-130.
Nikonenko, V., Lebedev, K., Manzanares, J.A. and Pourcelly, G. (2003), "Modelling the transport of carbonic acid anions through anion-exchange membranes", *Electrochim. Acta*, **48**(24), 3639-3650.
Palatý, Z. and Žáková, A. (2001), "Transport of hydrochloric acid through anion-exchange membrane NEOSEPTA-AFN. Application of Nernst–Planck equation", *J. Membrane Sci.*, **189**(2), 205-216.
Palatý, Z. and Žáková, A. (2003), "Transport of some strong incompletely dissociated acids through anion-exchange membrane", *J. Coll. Interf. Sci.*, **268**(1), 188-199.
Peeters, J.M.M., Boom, J.P., Mulder, M.H.V. and Strathmann H. (1998), "Retention measurements of nanofiltration membranes with electrolyte solutions", *J. Membrane Sci.*, **145**(2), 199-209.
Pisarska, B. and Dylewski, R. (2005), "Analysis of Preparation Conditions of H_2SO_4 and NaOH from Sodium Sulfate Solutions by Electrodialysis", *Russian J. Appl. Chem.,* **78**, 1288-1293.
Pourcelly, G., Tugas, I. and Gavach, C. (1994), "Electrotransport of sulphuric acid in special anion exchange membranes for the recovery of acids", *J. Membrane Sci.*, **97**(27), 99-107.
Prado-Rubio, O.A., Møllerhøj, M., Jørgensen, S.B. and Jonsson, G. (2010), "Modeling Donnan dialysis separation for carboxylic anion recovery", *Comp. Chem. Eng.*, **34**(10), 1567-1579.
Robinson, R.A. and Stokes, R.H. (1959), *Electrolyte Solutions*, Butterworths, London.
Scott, K. (1995), *Handbook of Industrial Membranes*, Elsevier Advanced Technology, Oxford.
Touaibia, D., Kerdjoudj, H. and Cherif, A.T. (1996), "Concentration and purification of wet industrial phosphoric acid by electro-electrodialysis", *J. Appl. Electrochem.*, **26**(10), 1071-1073.

RJ

Appendix

Calculation of mass fluxes and J_v

The mass fluxes through the membranes were calculated from the following formulae:

$$J_{mass,\mathrm{AM}} = \frac{1}{2S_m t}(\Delta m_{an} + \Delta m_{am} - \Delta m_{ca}) \tag{A1a}$$

$$J_{mass,\mathrm{BM}} = \frac{1}{2S_m t}(\Delta m_{an} - \Delta m_{am} - \Delta m_{ca}) \tag{A1b}$$

where

$$\Delta m_\alpha = m_{\alpha,t} + \sum_i m_{sam,\alpha,i} + n_F r_{F,\alpha} - m_{\alpha,0} \qquad \alpha = \mathrm{ca, am, an} \tag{A2}$$

$$r_{F,ca} \equiv \frac{1}{2} M_{\mathrm{H_2}} \qquad r_{F,am} \equiv x_{w,am} M_w - M_{\mathrm{H^+}} \qquad r_{F,an} \equiv \left(\frac{1}{2} - x_{w,am}\right) M_w \tag{A3a-c}$$

$x_{w,am}$ is the fraction of water splitted in BM, coming from the middle solution. Here, it is assumed that $x_{w,am} = 0.5$. n_F is the number of moles of the elementary charge passed through the system during the process. $r_{F,\alpha}$ is the change of the α solution mass resulting from electrode reactions and/or water splitting in BM caused by passing 1 F of charge. $m_{sam,\alpha,i}$ is the mass of i-th sample taken from the α solution. M_i is a molar weight of *i*-th species. Eqs. (A1a,b) result from the fact that Δm_α (α = ca, am, an) are not independent variables, *i.e.* there are 3 equations relating them with two independent variables $J_{mass,\mathrm{AM}}$ and $J_{mass,\mathrm{BM}}$:

$$\Delta m_{ca} = -J_{mass,AM} S_m t\,,\ \Delta m_{an} = J_{mass,BM} S_m t \text{ and } \Delta m_{am} = (J_{mass,BM} - J_{mass,AM}) S_m t \tag{A4a-c}$$

from which two different formulas for the calculation of each mass flux can be obtained. Using statistical methods (Brandt 1976) it can be shown that the best flux estimate is just an arithmetic mean of these formulas, *i.e.*

Eqs. (A1a,b). The volume flow through AM, J_v, was calculated from $J_{mass,AM}$ divided by the arithmetic mean of the densities of solutions on the both sides of AM.

Substituting (A2, A3) into (A1) it should be noticed that $J_{mass,MA}$ does not depend on the assumption about $x_{w,am}$. Only $J_{mass,AM}$ depends on that assumption. As $J_{mass,BM}$ insignificantly changes the composition of the middle solution, the assumption about $x_{w,am}$ has a negligible influence on the model calculations.

Calculation of the mean diffusion permeability coefficient $\langle P_{s,i}\rangle$,

The mean permeability coefficient $\langle P_{s,i}\rangle$, i = HCl or H_3PO_4, was calculated according to the method described in (Koter and Kultys 2008):

$$\langle P_{s,i}\rangle = \frac{1}{S_m t_r}\int_0^{t_r}\frac{1}{\Delta c_i}\frac{d(c_{i,d}V_{i,d})}{dt}dt \tag{A.5}$$

where t_r is the time of experiment. For the linear dependence of $c_{i,d}V_{i,d}$ on time, Eq. (A1) takes the form:

$$\langle P_{s,i}\rangle \approx \frac{1}{S_m t}\frac{d(c_{i,d}V_{i,d})}{dt}\sum_{j=1}^{r}\frac{1}{2}\left(\frac{1}{\Delta c_{i,j-1}}+\frac{1}{\Delta c_{i,j}}\right)\Delta t_j \tag{A.5a}$$

where $\Delta t_j = t_j - t_{j\text{-}1}$, $\Delta c_{i,j}$ is the concentration difference across the membrane observed at time t_j. It should be noted that in derivation of Eq. (A.5), no cross-effects related with the presence of other acid were taken into account.

List of symbols

c	concentration (mol m^{-3})
$c^{\ominus}$	standard concentration ($c^{\ominus}$ = 1 mol dm^{-3})
$\overline{c}_m$	concentration of fixed charges (mol m^{-3})
$\overline{c}_{m,\max}$	maximum concentration of fixed charges (mol m^{-3})
CE	current efficiency
D_i	diffusion coefficient of species i (m^2s^{-1})
F	Faraday constant (F = 96485 C mol^{-1})
j	electric current density (A m^{-2})
J_i	flux of species i (mol $m^{-2}s^{-1}$)
$J_{mass,AM}$	mass flow through the anion-exchange membrane (kg $m^{-2}s^{-1}$)
J_v	volume flux (m s^{-1})
$k_{DV\theta}$	porosity-tortuosity coefficient
K_α	thermodynamic equilibrium constant of reaction α
$K_{\alpha,c}$	concentration equilibrium constant of reaction α
l_m	thickness of membrane (m)
l_{pol}	thickness of polarization layer (m)
m	mass (kg)
m	molality (mol kg^{-1})
m'	concentration expressed in moles per kg of solution (mol kg^{-1})
$m_{sam,\alpha,i}$	mass of i-th sample taken from the α solution (kg),
M_i	molar weight of i-th species (kg mol^{-1})
n	number of moles (mol)
n_F	number of moles of elementary charge passed through the system, $n_F \equiv It/F$ (mol)
$P_{s,i}$	permeability of i-th acid (m s^{-1})
$r_{F,\alpha}$	change of mass of the a solution resulting from electrode reaction and/or water splitting in BM caused by passing 1 mole of elementary charge (kg mol^{-1})
R	gas constant (R = 8.314 J $K^{-1}mol^{-1}$)
S_m	area of membrane (m^2)
t	time (s)
t_i	transport number of ion i
T	temperature (K)
V	volume of solution (m^3)
V_p	volume fraction of membrane pores
x	coordinate of x-axis perpendicular to the surface of membrane (m)

$x_{w,am}$	fraction of water splitted in BM, coming from the middle solution
z_i	charge number of ion i
z_m	charge number of fixed charges
θ	tortuosity coefficient of membrane pores
ρ	density (kg m^{-3})
φ'	dimensionless electric potential ($\varphi' = \varphi F/RT$).

Subscripts

0 – $t = 0$, 1 – H^+, 2 – Cl^-, 3 – $H_2PO_4^-$, 4 – $H_5P_2O_8^-$, 5 – H_3PO_4, am – middle solution (between AM and BM membranes), an – anode solution, b – bulk, c – concentrated, ca – cathode solution, d – diluted, m – membrane, A – H_3PO_4 or $H_2PO_4^-$, bar over the symbol denotes the solution in membrane pores.